Proceedings of 2005 5th IEEE Conference on Nanotechnology
Nagoya, Japan, July 2005

Growth and characterization of vertically aligned 1D IrO_2 nanocrystals via reactive sputtering

A. V. Korotcov[1], Y. S. Huang[1,*], D. S. Tsai[2], and K. K. Tiong[3]

[1] Department of Electronic Engineering, National Taiwan University of Science and Technology, Taipei, 106, Taiwan

[2] Department of Chemical Engineering, National Taiwan University of Science and Technology, Taipei, 106, Taiwan

[3] Department of Electrical Engineering, National Taiwan Ocean University, Keelung, 202, Taiwan

[*] Corresponding author. Tel.: + 886-2-2-737-6385; fax: +886-2-2-737-6424;
e-mail: ysh@et.ntust.edu.tw

***Abstract* — We report the preparation of 1D vertically aligned IrO_2 nanocrystals on $LiNbO_3$ (100) substrates by reactive magnetron sputtering with Ir metal target. The effects of sputtering conditions such as pressure, rf power, substrate temperature etc. have been presented and discussed. The surface morphology, structural and spectroscopic properties of the as-grown nanocrystals have been characterized using field-emission scanning electron microscopy (FESEM), X-ray diffractometry (XRD) and micro-Raman scattering. The red-shift and asymmetric broadening of Raman lineshape have been analyzed and attributed to both the size effect and residual stress.**

***Index Terms* — Iridium dioxide, reactive sputtering, Field emission scanning electron microscopy, Raman scattering, X-ray spectroscopy.**

I. INTRODUCTION

Recently, one-dimensional (1D) nanocrystals (NCs) such as wires, rods, belts and tubes have become the focus of intensive research owing to their interest in fundamental physics and unique application in nanoscale device fabrication [1]. Vapor-phase synthesis is probably the most extensively explored approach to the formation of 1D NCs. From the main principles of formatting 1D NCs, it is possible to process any solid material into 1D nanostructures by controlling the supersaturation at a relatively low level. The dimensions of the 1D NCs can be varied by controlling a number of parameters that include the supersaturation factor, nucleation size and growth rate.

Iridium dioxide (IrO_2) is a representative rutile-type conductive oxide. Single crystalline IrO_2 shows metallic behavior (~40 μΩ-cm at room temperature for polycrystalline sputtered film) in electrical and optical properties [2-4]. Owing to the conductive nature, high thermal and chemical stability, effective diffusion barrier for oxygen, IrO_2 1D nanostructures have been an attractive material for field emitters, sensors, displays, interconnects and etc. [5-7].

Metal-organic chemical vapor deposition (MOCVD) has been successfully employed for the growth of IrO_2 1D NCs on different substrates [8]. However, MOCVD, a technique, generally requires multiple processing steps to fabricate nanostructures. On the other hand, reactive rf magnetron sputtering has several advantages including a single deposition step to obtain the nanostructures and better control of the growth conditions.

In this work, we report the deposition of 1D vertically aligned IrO_2 NCs by reactive sputtering using an Ir metal target. The surface morphology, structure and spectroscopic properties of the as deposited NCs are investigated. The effects of sputtering conditions such as pressure, rf-power, and temperature of substrate are discussed. The red-shift and asymmetric broadening of Raman lineshape have been analyzed and attributed to both the size effect and residual stress.

II. EXPERIMENTAL DETAILS

The investigation was performed using a home-made high vacuum rf magnetron sputtering system. A schematic diagram of the system is shown in Fig. 1. The sputtering gun has a standard circular planar magnetron. The sputtering target was 1-inch of Ir (99.95%) metal. IrO_2 structures were deposited on the $LiNbO_3$ (LNO) (100) substrates (~10×10mm^2). Substrates were cleaned consecutively with acetone and methanol in an ultrasonic

0-7803-9199-3/05/$20.00 ©2005 IEEE

bath for 10 min to prevent any contamination of the substrate surface.

The sputtering chamber was maintained at a base pressure of ~ 3×10^{-5} mbar. Reactive sputtering was carried out in O_2 atmosphere at different sputtering pressure and in the range from 2×10^{-2} mbar to 9.5×10^{-2} mbar. The degree of surface mobility of the deposited atoms was varied via adjusting the power of rf-generator in the range 55-72 W and distance between the gun and substrate from 33 mm to 100 mm. The substrate temperature was kept constant during the sputtering process and was set at different value between 250 °C and 450 °C. The period for each sputtering was 30 min or 60 min. The sputtering conditions are listed in Table 1.

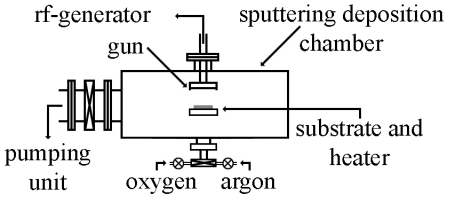

Fig. 1. Schematic diagram of the sputtering system.

TABLE I
SPUTTERING CONDITIONS

target	1- inch Ir (99.95%)
substrate	$LiNbO_3$ – (100)
target-substrate distance	33 – 100 mm
rf-power	55 – 72 W
background pressure	3×10^{-5}mbar
sputtering pressure	2×10^{-2}mbar – 9.5×10^{-2}mbar
DC-bias	~ 480V
substrate temperature	250 – 450°C

The morphology of the IrO_2 1D NCs was recorded using a JEOL-JSM6500F field-emission scanning electron microscope (FESEM). The dimensions and growth rates of various IrO_2 samples were estimated with the 90° cross-sectional FESEM images. Crystal structures were determined by X-ray diffraction (XRD). XRD patterns were taken on a Rigaku D/Max-RC X-ray diffractometer. Raman spectra were recorded at room temperature utilizing the back scattering mode on a Renishaw inVia Raman microscope system. The system is equipped with an optical microscope for focusing the 514.5 nm excitation line from the Ar-ion laser beam onto the sample.

III. RESULTS AND DISCUSSION

Under the growth conditions as specified by Table 1, we found that the obtained NCs as indicated by the FESEM images have a wedge-shaped geometry and almost all of them have sharp tips. The diameters (D) of the NCs can vary from 20 nm to 100 nm depending on the growth conditions. A thorough investigation of the as-grown NCs showed that optimum growth conditions are L_g = 45 mm, T_s = 400°C, sputtering pressure P = 6.5 ± 0.1×10^{-2} mbar, DC-bias = 480 V and rf magnetron power = 65 W. The FESEM images of the NCs grown under the optimum conditions are depicted in Fig. 2. The estimated diameter D, length and packing density of NCs are around ~ 40 nm, ~ 350 nm and 350 μm^{-2}, respectively.

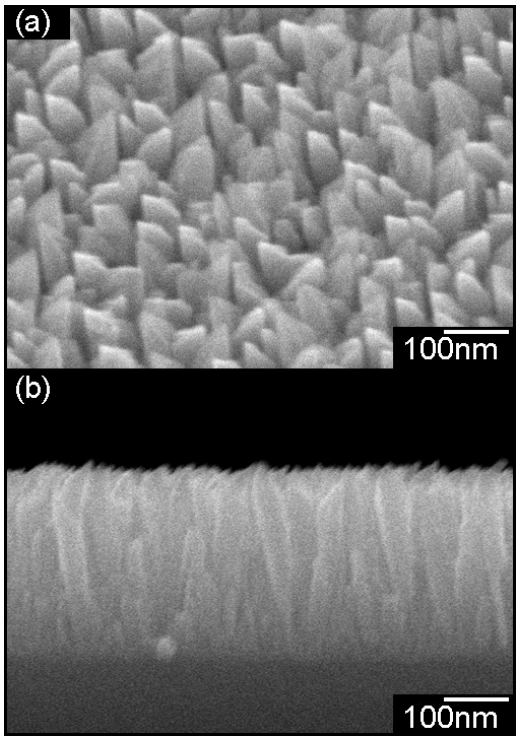

Fig. 2. FESEM images of the IrO_2 1D nanostructures on LNO (100) deposited at P=$6.5\text{x}10^{-2}$mbar, RF-power=65W, L_g= 45mm, T_S=400°C, t_d=30min. (a) – 30° perspective-view; (b) –cross section view)

XRD patterns of the as-grown NCs showed well aligned NCs along [001] direction as illustrated in Fig. 3(a). Deviation from the optimum conditions showed the formation of NCs with a small degree of (301) orientation as demonstrated in Fig. 3(b), where the growth conditions are L_g = 45 mm, T_s = 350 °C, sputtering pressure P = 5.5 ± 0.1×10^{-2} mbar, DC-bias = 480 V and rf magnetron power = 72 W. The XRD patterns reveal two peaks, a prominent peak at 58.47° and a weak feature at ~ 69.3°, corresponding respectively, to reflections from IrO_2 (002) and (301). The intensity ratio I(002)/I(301) was estimated to be 65. If we look closely at the inset in Fig. 3(a), we

notice that the weak signal at 69.3° appeared as a weak asymmetric shoulder superimposed on the prominent LNO (300) signal. The intensity ratio I(002)/I(301) was estimated to be ~ 1000.

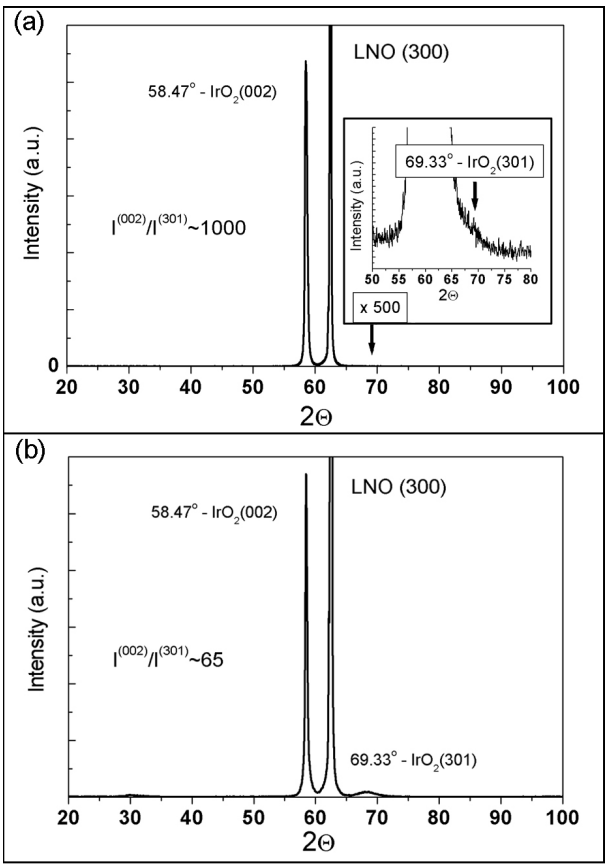

Fig. 3. X-ray diffraction patterns of the IrO_2 NCs on LNO (100) deposited at: (a) P=6.5x10^{-2}mbar, rf power=65W, L_g= 45mm, T_S=400°C, t_d=30min; (b) P=5.5x10^{-2}mbar, rf power=72W, L_g= 45mm, T_S=350°C, t_d=60min.

These results indicate that the IrO_2 NCs wedge-shaped standing on substrate are perfectly vertical and follows the substrate LNO (100) orientation. Growth with (001) orientation of IrO_2 on LNO (100) substrates can be described based on the lattice relationship. Lattice misfit at the interface produces strain energy when the IrO_2 is nucleated. The orientation that minimizes the lattice misfit and produces the smallest strain energy will be preferred. The schematic plots of the relationships of IrO_2 (001)//$LiNbO_3$ (100) is depicted in Fig. 4. This growth pattern results in the smallest lattice mismatch between the IrO_2 NCs and substrates. The lattice parameters are a = b = 0.449 nm and c = 0.315 nm for IrO_2 and a = b = 0.515 nm and c = 1.386 nm for $LiNbO_3$ [9]. According to the plots, the in-plane orientation of IrO_2 [100] along of LNO [001] shows a mismatch ~ 12.8% and for IrO_2 [010] along LNO [001] ~ 30-40%. Moreover, the assumption of the lattice mismatch being the factor can explain the generation of the two preferential orientations (001) and (301) of reactive sputtered IrO_2 1D nanostructures, with (001) orientation being dominant.

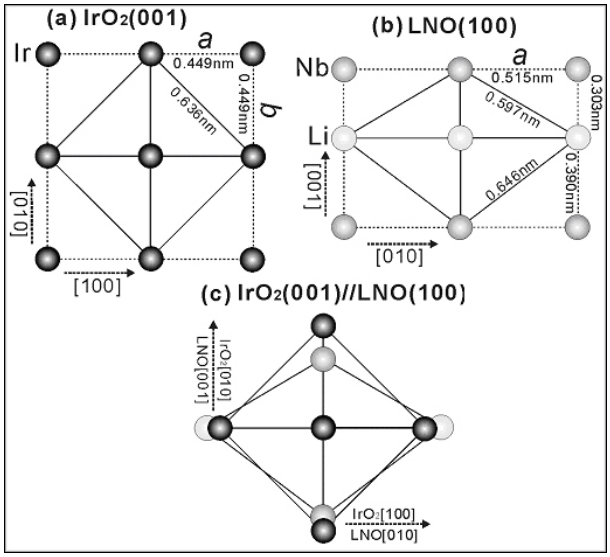

Fig. 4. The schematic drawing of the relationship between IrO_2 and $LiNbO_3$: (a) IrO_2 (001) plane; (b) $LiNbO_3$ (100) plane; (c) IrO_2 (001) on $LiNbO_3$ (100).

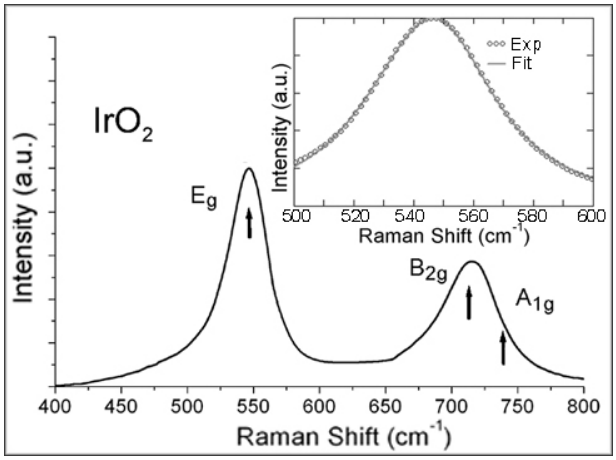

Fig. 5. Raman spectra of the IrO_2 1-D nanostructures on LNO (100) in the range of E_g, B_{2g} and A_{1g} modes. In the insert is shown theoretical results of analyze of the lineshape using spatial correlation model (solid line). P=6.5×10^{-2}mbar, T_s=400°C, L_g=45mm, t_d=30min.

The first-order Raman spectra of the reactive sputtered IrO_2 NCs were used to extract the structural information (Fig. 5). Three Raman modes, identified as E_g, B_{2g}, and A_{1g} were observed in the vicinity of 561 cm^{-1}, 728 cm^{-1},

752 cm^{-1} (peak positions from single crystal [10]). Since the intensity of the E_g mode is much larger than of the other two modes we will focus our analysis on this mode. We analyzed our results using the spatial correlation (SC) model of Campbell and Fauchet [11]. For the dispersion relation, $\omega(q)$ we took the analytical model relationship based on a one-dimensional linear-chain model [9].

The Raman spectrum of the reactive sputtered IrO_2 NCs reveals a total of 14.6 cm^{-1} red-shift in the peak position (E_g at 546.4cm^{-1}) and an asymmetric broadening, full width at half-maximum (FWHM) of 46 cm^{-1} as compared with the single crystal case of FWHM = 12cm^{-1}. Using the diameter D ~ 40 nm, estimated from FESEM images, as the correlation length in the SC model, we have compute the red shift as a result of the phonon confinement effect to be 7 cm^{-1}. It is noted that an additional red shift of ~ 8 cm^{-1} is needed to account for the change in the Raman feature. Our analysis showed that a red shift induced by a residual stress has to be included in the SC model in order to explain satisfactorily the red shift and asymmetric line width broadening of the observed Raman signal of the E_g mode. It is emphasized that the modification of the SC model should be substrate dependence and also depends on the morphology of the NCs. For instance, solid rods and tubes on the same substrate will experience differing residual stress. Our propose modification of the SC model, by including the stress induced shift, in analyzing the observed Raman features can be utilized as a useful method for the detection and estimation of the residual stress in the 1D nanostructures.

IV. Conclusion

We have demonstrated successful growth of well aligned highly uniform IrO_2 1D NCs using a home-made high vacuum rf magnetron sputtering system. The structure and morphology of IrO_2 reactive sputtered 1D NCs strongly depends on sputtering conditions: sputtering pressure, distance between gun and substrate, power of rf magnetron gun and temperature of substrate. Two orientations of IrO_2 nanostructures, namely, (001) and (301) can be observed depending on the growth conditions. The content of (301) orientation can be almost eliminated by tuning the growth conditions to the optimum condition: rf power = 65W, sputtering pressure P = 6.5×10^{-2} mbar, substrate temperature T_s = 400°C, target-substrate distance L_g = 45 mm and DC-bias = 480 V.

The micro-Raman spectrum of the reactive sputtered IrO_2 NCs reveal 14.6 cm^{-1} red-shift in the peak position of E_g mode at 546.4 cm^{-1} and an asymmetric broadening of 46 cm^{-1}. The observed Raman line shape can be explained satisfactorily by the proposed modified SC model which includes an additional stress induced red shift of ~ 8 cm^{-1}. Our propose modification of the SC model, by including the stress induced shift, in analyzing the observed Raman features can be utilized as a useful method for the detection and estimation of the residual stress in the 1D nanostructures.

Acknowledgement

The authors acknowledge the support of the National Science Council of Taiwan under the projects No. NSC93-2120-M-011-001 and No. NSC93-2112-M-019-005.

References

[1] Y. Xia, P. Yang, Y. Sun, Y. Wu, B. Mayers, B. Gates,Y. Yin, F. Kim, H. Yan, "One-dimentional Nanostructures: Synthesis, Characterization and Application", Advanced Materials, vol. 15, no. 5, pp. 353-389, 2003

[2] C. U. Pinnow, I. Kasko, C. Dehm, B. Jobst, M. Seibt, U.Geyer, "Preparation and properties of dc-sputtered IrO_2 and Ir thin films for oxyden barrier applications in advanced memory technology", J. Vac. Sci. Technol., vol. B19, no. 5, pp. 1857-1865, 2001.

[3] R. H. Horng, D. S. Wuu, L. H. Wu, M. K. Lee, "Formation process and material properties of reactive sputtered IrO_2 thin films", Thin Solid Films, vol. 373, no. 1, pp. 231-234, 2000.

[4] P. C. Liao, W. S. Ho, Y. S. Huang, K. K. Tiong, "Characterization of sputtered iridium dioxide thin films", J. Mater. Res., vol. 13, no. 5, pp. 1318-1326, 1998.

[5] B. R. Chalamala, Y. Wei, G. Rossi, B. G. Smith, R. H. Reuss, "Fabrication of iridium field emitter arrays", Appl. Phys. Lett., vol. 77, pp. 3284-3286, 2000.

[6] Y. Kuratani,Y. Morikawa, M. Okuyama, "Improvement of field-enduced electron emission using Ir or IrO_2 electrode and ferroelectric film coating", Jpn. J. Appl. Phys., vol. 37, pp. 5421-5423, 1998.

[7] D. Chiang, P. Z. Lei, F. Zhang, R. Barrowcliff, "Dynamic EFM spectroscopy studies on electric force gradients of IrO_2 nanorod arrays", Nanotechnology, vol. 16, pp. 35-40, 2005.

[8] R. S. Chen, H. M. Chang, Y. S. Huang, D. S. Tsai, K. C. Chiu, "Morphological evolution of the self-assembled IrO_2 one-dimntional nanocrystals", Nanotechnology, vol. 16, pp. 93-97, 2005.

[9] R. S. Chen, H. M. Chang, Y. S. Huang, D. S. Tsai, S. Chattopadhyay, K. H. Chen, "Growth and characterization of vertically aligned self-assembled IrO_2 nanotubes on oxide substrates", J. Cryst. Growth, vol. 271, pp. 105-112, 2004.

[10] Y. S. Huang, S. S. Lin, C. R. Huang, M. C. Lee, T. E. Dann, F. Z. Chien, "Raman spectrum of IrO_2", Solid State Commun, vol. 70, pp. 517-522, 1989.

[11] I. H. Campbell and P. M. Fauchet, "The effects of microcrystal size and shape on the one phonon raman spectra of crystalline semiconductors", Solid State Communications, vol. 58, no. 10, pp. 739-741, 1986.